

An annealing study of the R1 EPR centre (the nearest-neighbour di-⟨100⟩-split self-interstitial)
in diamond

This article has been downloaded from IOPscience. Please scroll down to see the full text article.

2001 J. Phys.: Condens. Matter 13 2045

(<http://iopscience.iop.org/0953-8984/13/10/301>)

View [the table of contents for this issue](#), or go to the [journal homepage](#) for more

Download details:

IP Address: 171.66.16.226

The article was downloaded on 16/05/2010 at 08:46

Please note that [terms and conditions apply](#).

An annealing study of the R1 EPR centre (the nearest-neighbour di- $\langle 100 \rangle$ -split self-interstitial) in diamond

D J Twitchen^{1,3}, M E Newton^{1,4}, J M Baker¹, T R Anthony² and W F Banholzer²

¹ Oxford Physics, Clarendon Laboratory, Parks Road, Oxford OX1 3PU, UK

² General Electric Company, Corporate Research and Development, Schenectady, NY, USA

E-mail: d.twitchen1@physics.oxford.ac.uk, mark.newton@kcl.ac.uk and m.baker1@physics.oxford.ac.uk

Received 4 October 2000

Abstract

Results are reported of both isochronal and isothermal annealing studies of the R1 EPR centre (known to be a pair of parallel nearest-neighbouring $\langle 100 \rangle$ -split self-interstitials) produced by 2 MeV electron irradiation of synthetic type IIa diamonds of very low defect concentration before irradiation. The annealing out of R1 is not associated with any overall change in the concentration of isolated vacancies or interstitials. The isothermal decay corresponds to a first-order process with a rate constant conforming to an Arrhenius relationship with activation energy 0.6(1) eV and an unusually low attempt frequency. That the activation energy is much lower than the migration energy of isolated interstitials (1.68(15) eV) is taken to indicate that it corresponds to a combination of the energy required to excite R1 into an $S = 0$ state and that required to translate one of the split interstitials over the potential barrier into the next lattice site. This process may be linked to an associated rise in the concentration of the 3H (2.462 eV) optical defect; but the precise relationship between the diamagnetic site formed by the decay of R1 and the 3H optical centre is not revealed by this study.

1. Introduction

Ever since Crookes irradiated diamond in 1904 with α -particles emitted from radium [1], radiation damage in diamond has been a topic of detailed investigation. The processes of migration and agglomeration of defects and their interaction with substrate impurities have attracted attention for both fundamental and technological reasons as regards features such as

³ Present address: De Beers Industrial Diamonds (UK) Ltd, Ascot, UK.

⁴ Present address: Department of Physics, King's College London, Strand, London WC2R 2LS, UK.

the evolution of defects and accumulation of damage during ion implantation, the formation of secondary defects and transient-enhanced diffusion.

Recently there has been considerable progress in the identification of simple, interstitial-related defects in crystalline diamond. Electron paramagnetic resonance (EPR) studies of electron-irradiated synthetic diamond grown at high temperature and pressure (HTP) with $^{12}\text{C}:^{13}\text{C}$ in the ratios 99.999:1, 50:50 and 95:5, using the technique described in reference [2], have resulted in the identification of the $\langle 100 \rangle$ -split self-interstitial in the neutral charge state I^0 (R2 EPR centre) [3], the di- $\langle 100 \rangle$ -split self-interstitial $(\text{I}-\text{I})^0$ (R1 EPR centre; see figure 1(a)) [4] and the O3 EPR defect which contains three interstitials [5]. R1 and R2 centres are observed in all type II (< 1 part per million carbon atoms of nitrogen impurity) and type I (nitrogen content detectable by infrared absorption) diamonds after neutron or electron irradiation. The details of the mechanisms of the formation and decay of centres incorporating multiple interstitial atoms are still unclear.

The analysis of optical and EPR spectra can give information about the molecular models of intrinsic point defects, but to understand the mechanisms of their creation, diffusion, interaction and modification requires study of the conditions of their creation and the effect of external influences such as impurities, irradiation, illumination and annealing. Rates of production by 2 MeV electron irradiation have recently been measured [6, 7]. In an attempt to elucidate some of these processes, we present the results of two annealing studies of the EPR centre R1 (shown in figure 1(a)) in electron-irradiated synthetic type IIa (very low nitrogen concentration) diamond.

Several previous studies have been reported of isochronal annealing of the defects produced in diamonds by irradiation with energetic electrons or neutrons [8]. The annealing behaviour of the vacancy is relatively well understood. The vacancy has been studied for the neutral state (V^0) via the optical GR1 zero-phonon line (ZPL) at 1.673 eV [9] and EPR of an excited $^5\text{A}_2$ state [10], and for the negative state (V^-) via both optical spectra (ZPL at 3.149 eV) [11] and EPR spectra (S1 and S2 centres) [12]. It is thought that vacancies migrate in the neutral charge state (V^0) at 900 K, with an activation energy of 2.3(3) eV [13]. Some loss of vacancies at lower temperatures (700–800 K), when the vacancy is not mobile, is thought to be due to recombination with mobile self-interstitials; the activation energy for the process

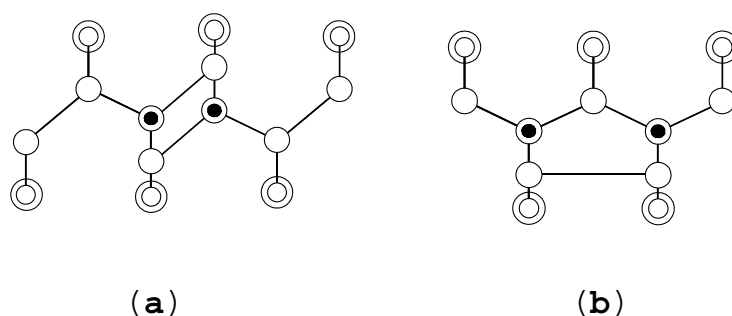


Figure 1. Defects in diamond comprising two parallel $\langle 100 \rangle$ -split self-interstitials lying in a $\{110\}$ plane, (a) at nearest-neighbour sites (R1) and (b) at next-nearest-neighbour sites. The diagram shows a projection onto the $\{110\}$ plane, single circles representing atoms in this plane and double circles atoms $(1/\sqrt{8})a_0$ above and below the plane. The singly occupied non-bonding p_π orbitals are indicated by black circles at the centre of the atoms. These figures are stylistic to emphasize the position of the $\langle 100 \rangle$ -split interstitials: in the actual structure the orientation of these split interstitials changes to give more like a square set of bonds in (a) and a pentagonal set of bonds in (b), together with some dilatation of the nearby atoms.

is 1.68(15) eV [14]. The R1 and R2 EPR defects anneal out in the ranges 620–670 K and 670–730 K respectively. The annealing of R2 in this temperature range has been interpreted as indicating that it is this range where I^0 becomes mobile, and where some of the I^0 recombine with some of the vacancies [3].

These earlier annealing measurements have been made using the isochronal step-annealing method in which the sample is held for a fixed time at successively higher temperatures, but is returned to room temperature or below for measurement. We have made new isochronal annealing measurements on these defects in HTP synthetic diamond with a much lower impurity and defect density than those previously reported, and also isothermal annealing measurements where the EPR of the defect is monitored as a function of time at a pre-set temperature. It is the high purity of the samples that is essential to allowing the investigation of intrinsic properties.

2. Experimental procedure

Two single-crystal synthetic diamonds grown at high temperature and pressure (HTP) by the temperature gradient method were used in this study. Sample A, which was used in the isothermal annealing, was laser cut and polished (to allow optical measurements) into four pieces (A1–4), of approximate dimensions $2 \times 2 \times 0.5$ mm prior to being irradiated. Sample B, of dimensions $4.5 \times 2.5 \times 1$ mm, was used for isochronal annealing. The samples were characterized using EPR, infrared, visible and UV optical absorption measurements before and after electron irradiation.

The samples were irradiated at nominally room temperature, on a water-cooled copper plate, using 1.9 MeV electrons and a beam current of $15 \mu\text{A cm}^{-2}$. Irradiations of samples A1–4 were done simultaneously to a dose of $2 \times 10^{18} \text{ cm}^{-2}$, and of sample B to a dose of $6.5 \times 10^{17} \text{ cm}^{-2}$. After irradiation, in addition to V^0 , the R1 and R2 centres were found in both samples.

EPR measurements were made with a standard EPR spectrometer and a high- Q water-cooled TE_{011} cylindrical cavity. The sample was placed in a quartz Dewar which was inserted into the centre of the cavity. The temperature of the gas passing through the Dewar was controlled by a high-power temperature controller. Temperatures between 100 and 1200 K are attainable with this system. The temperature stability of the water-cooled cavity was essential to allow measurement of the EPR signal during isothermal anneals that lasted over 10 hours. The overall stability of the EPR system was monitored by using a reference sample that was placed in the cavity, but outside the Dewar. Using this reference, any change in EPR sensitivity due to variations in overall spectrometer performance with time could be corrected for.

3. Results

3.1. Isothermal annealing

For a sample held at 440 K the R1 EPR signal showed no time dependence, but measurements of the isothermal decay of the R1 centre between 10 and 600 minutes were made at 456 (twice), 498, 532 and 599 K, showing a slow exponential decay. Figure 2(a) shows the data for the decay of [R1], the concentration of R1, measured at 559 K as a function of time t , and the fit to the relation

$$[\text{R1}]_t = [\text{R1}]_0 \exp\{-r_T t\} \quad (1)$$

where $[\text{R1}]_0$ is the concentration of R1 at time $t = 0$, the starting time of the measurements when the temperature and spectrometer were stable. Figure 2(b) shows that the rate of this

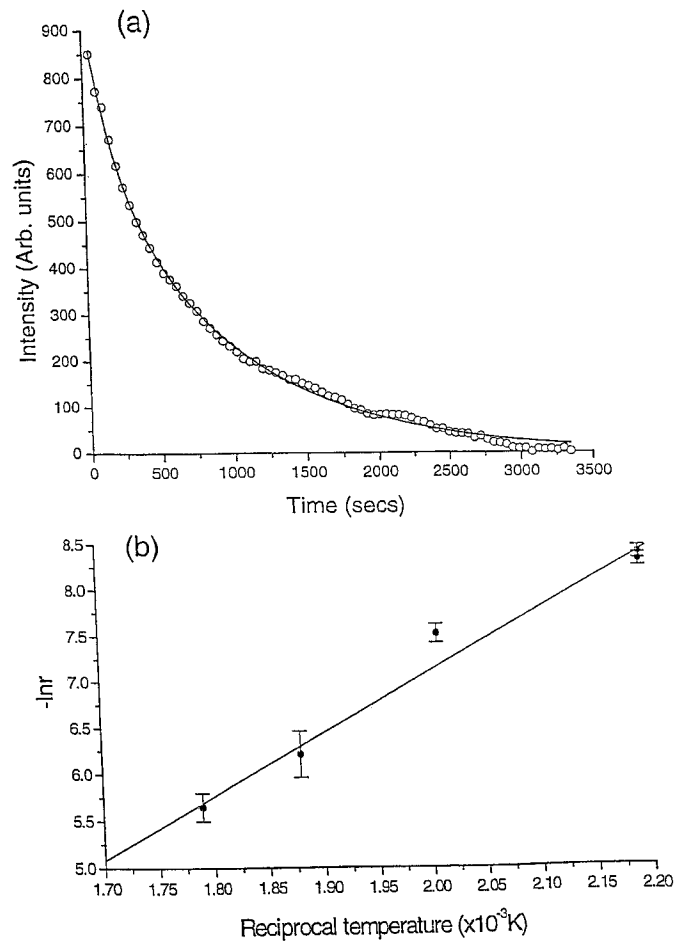


Figure 2. (a) Experimental points (circles) showing the decrease in the intensity of R1 in sample A3 during annealing at 559 K. For the isothermal annealing, the EPR spectrometer, operating at ~ 9.6 GHz, was set on the R1 line for an external magnetic field ~ 362 mT along (100). The line through the points in the figure shows the fit to first-order kinetics. The error bars are of the order of the size of the symbols. (b) An Arrhenius plot of the measured time constant $(r_T)^{-1}$ of the decay of the concentration of R1 on annealing, such as that shown in (a). The line shows a fit to equation (2) with $E_{01} = 0.6(1)$ eV and $r_{01} \sim 10^3$ s $^{-1}$.

process can be fitted to the Arrhenius relation

$$r_T = r_{01} \exp(-E_{01}/kT) \quad (2)$$

where r_{01} is a characteristic rate for the process and E_{01} is the associated activation energy: the fitted line corresponds to $E_{10} = 0.6(1)$ eV and r_{10} is 10^3 s $^{-1}$, the uncertainty in r_{10} being at least a factor of 10.

3.2. Isochronal annealing

Figure 3 shows the measured concentrations of several relevant EPR and optical defects in sample B after isochronal annealing. Optical absorption measurements were made at 77 K over the energy range 1.6 to 5.5 eV. The isochronal annealing curve for R1 in sample B is

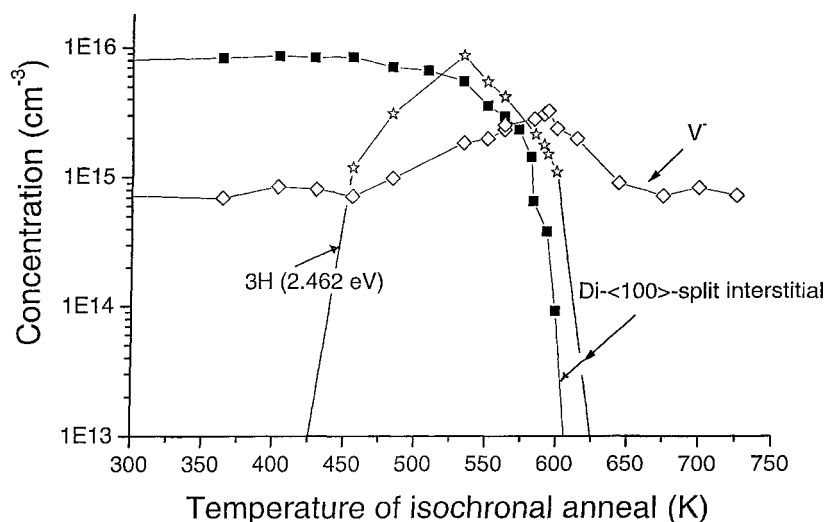


Figure 3. Isochronal annealing of the EPR of the di- $\langle 100 \rangle$ -split self-interstitial (R1), the negative vacancy (V^-) and the 2.46 eV line of the 3H defect, measured for sample B. The annealing time was 65 minutes. The plot for 3H is placed arbitrarily on the concentration axis, as the oscillator strength of the 2.45 eV line is unknown. The total concentration of neutral vacancies (V^0), measured via the 1.673 eV line, remained constant in the temperature interval shown.

similar to those measured by other workers [8]. There is an increase in the concentration of V^- in the temperature range where R1 is annealing out, which is just below the noise level for observation of any corresponding decrease in V^0 . However, the overall effect of the complete removal of R1 is to leave the concentrations of V^0 and V^- unchanged. A change in the absorption strength of the 3H ZPL was detected during the annealing (figure 3); however, no other change of the optical or EPR spectrum was observed to correlate with the isochronal annealing curves shown in figure 3.

4. Discussion

4.1. The annealing mechanism

The activation energy of the process described by equation (2), 0.6(1) eV, is much smaller than the migration energy of the self-interstitial, 1.68(15) eV [13], and I^0 is not mobile at the temperature of measurement. The pre-factor, $\sim 1000 \text{ s}^{-1}$, is unexpectedly small for the usual type of attempt frequency for surmounting a potential barrier (typically $\sim 10^{13} \text{ s}^{-1}$).

The other important features of the process are that (a) there is no reduction in the number of vacancies shown by the GR1 absorption, (b) there is no indication of the production of isolated I^0 as monitored by the EPR of R2 and (c) the change is permanent. This suggests that the mode of decay of $(I-I)^0$ is not by its dissociation; but, nevertheless, there is a clear structural change. The simplest structural change without involving the production of I is that the interstitials move apart to form the defect I-C-I with parallel I, first proposed by Humble [15]. This is shown in figure 1(b), with two parallel p_z orbitals. Theoretical modelling shows this to be stable with $S = 0$ [16]. The suggested thermally stimulated transition during annealing between $(I-I)^0$ and $(I-C-I)^0$ would be inhibited by the change of spin from $S = 1$ to $S = 0$. However, it is known, from optically stimulated changes in the EPR spectrum, that R1

has an excited state in the band gap [17]. It is possible that the rather small activation energy for the annealing process, and the very low attempt frequency, are related to the energy needed to excite R1 into an $S = 0$ state before it can make the vibrationally assisted jump to the new configuration.

4.2. The relationship with 3H

The defect I–C–I, with C_{2v} symmetry, has not been identified: it would exhibit no EPR in its ground state, but it is expected to be optically active. It is possible that the optical defect 3H [18], which has the required rhombic I symmetry [19], and which becomes observable as R1 anneals out (the absorption of the 3H line at 2.46 eV also shown in figure 3), might correspond to this defect. Our data show that 3H in turn anneals out between 280 and 400 °C (550 and 670 K) (the same interval over which the concentration of V^- is increased). R2 begins to anneal out above about 670 K and hence I^0 becomes mobile.

It should be stressed that the absolute concentration of the defect which gives rise to 3H is not known. The data merely show that the peak of 3H corresponds to the loss of $\sim 30\%$ of the initial concentration of R1, and occurs at a different temperature (~ 70 K lower) from the peak in V^- , which corresponds to almost total loss of R1. The shapes of the isochronal annealing curves for 3H and V^- show that complex processes are going on. For a simple, single process of annealing out, the percentage loss after successive anneals to the *same* temperature would be the same, so annealing to successively higher temperature should produce increasingly greater falls at each step, as is observed for R1. That the curves for 3H and V^- do not become ever steeper indicates creation as well as decay. Also the equality of concentration of V^- before and after the peak suggests a steady background population to which other processes are adding and removing a separate transient population, which like that of 3H shows an increase followed by complete annealing out. Previous measurements on the annealing of 3H have shown decay at 900 K [20], which suggests that the 3H created in our measurements has a different mode of decay. Alternatively, the changes observed in the concentration of 3H could be due to charge transfer without any changes in the structural unit of the defect.

Previously 3H has been associated with the self-interstitial, probably in a negative charge state I^- , as it is produced abundantly by electron irradiation in a 300 keV TEM, and its presence outside the irradiated area indicates diffusion under the conditions of the irradiation [21]. In a sample where 50% of the carbon has been substituted for with ^{13}C , the local mode 280 meV above the ZPL of 3H shows a 1:2:1 isotope shift characteristic of a defect containing two equivalent carbon atoms. These measurements have been interpreted as showing that 3H corresponds to an isolated I [22]. However, since then, the EPR defect R2 has been shown unambiguously to be I^0 , and that does not exhibit luminescence characteristic of 3H [3]. One would expect I^- also to exhibit EPR with $S = \frac{1}{2}$, but no EPR centre has been associated with it, though it might be difficult to resolve it from other centres with $S = \frac{1}{2}$ if it were in low concentration. The isotope shift in 3H could indicate the association of I in I–C–I, where the isotope shift could be characteristic of the vibration of one of the sets of two identically bonded carbon atoms in the structure.

What happens when 3H anneals out in our samples is not clear. It is close to the temperature at which R2 begins to anneal out, I^0 becomes mobile and some vacancies disappear, which might be expected if 3H is I^- , but this is not consistent with the higher annealing temperature measured previously. If 3H corresponds to $(\text{I–C–I})^0$, it is possible that 3H breaks up into its constituent I, or that the two constituent I can diffuse together by successively changing their relative position, until they collide with a similar defect, with which they can combine to form a particularly stable ring of four I, linked by four bonds in a defect (I_4) with D_{2d} symmetry.

Although such a centre has been shown to be stable theoretically with $S = 0$, and is predicted to occur in silicon [23], it would not exhibit EPR, and no optical defect has yet been associated with it. The existence of O3 [5], $(\text{I-C-I-C-I})^0$, with a right-angle bend between the two I-C-I fragments, supports the existence of $(\text{I-C-I})^0$ as a precursor, and the low annealing temperature of O3 (700 K) may indicate capture of a further I to form I₄. If this model is correct, it is not clear why the annealing temperature of 3H is significantly different in our measurements from previous measurements. Much more work is needed to clarify the model for 3H, and if 3H is not $(\text{I-C-I})^0$, to find evidence of the latter.

5. Conclusions

Our data on the isothermal annealing of R1 (two nearest-neighbouring parallel $\langle 100 \rangle$ -split self-interstitials, $(\text{I-I})^0$), following an Arrhenius relation with an activation energy of 0.6 eV, significantly lower than the activation energy for diffusion of the self-interstitial, suggests that the annealing process does not correspond to dissociation into the constituent I and rapid migration apart, but proceeds by one of the constituent I moving to the next-nearest-neighbour position.

References

- [1] Crookes W 1904 *Proc. R. Soc. A* **74** 47
- [2] Bray J W and Anthony T R 1991 *Z. Phys. B* **84** 51
- [3] Hunt D C, Twitchen D J, Newton M E, Baker J M, Anthony T R, Banholzer W F and Vagarali S S 2000 *Phys. Rev. B* **61** 3863
- [4] Twitchen D J, Newton M E, Baker J M, Tucker O D, Anthony T R and Banholzer W F 1996 *Phys. Rev. B* **54** 6988
- [5] Hunt D C, Twitchen D J, Newton M E, Baker J M, van Wyk J A, Anthony T R and Banholzer W F 2000 *Phys. Rev. B* **62** 6587
- [6] Twitchen D J, Hunt D C, Newton M E, Baker J M, Anthony T R and Banholzer W F 1999 *Physica B* **273+274** 628
- [7] Twitchen D J, Hunt D C, Wade C, Newton M E, Baker J M, Anthony T R and Banholzer W F 1999 *Physica B* **273+274** 644
- [8] Ammerlaan C J A 1990 *Landolt-Börnstein New Series Group III*, vol 22b, ed M Schultz (Berlin: Springer) p 205 (figure 15)
- [9] Clark C D, Ditchburn R W and Dyer H B 1956 *Proc. R. Soc. A* **237** 75
- [10] van Wyk J A, Tucker O D, Newton M E, Baker J M, Woods G S and Spear P 1995 *Phys. Rev. B* **52** 12 657
- [11] Davies G 1977 *Phys. Chem. Carbon* **13** 1
- [12] Isoya J, Kanda H, Uchida Y, Lawson S C, Yamasaki S, Itoh H and Morita Y 1992 *Phys. Rev. B* **45** 1436
- [13] Davies G, Lawson S C, Collins A T, Mainwood A and Sharp S J 1992 *Phys. Rev. B* **46** 13 157
- [14] Allers L, Collins A T and Hiscock J 1998 *Diamond Relat. Mater.* **7** 228
- [15] Humble P 1982 *Proc. R. Soc. A* **381** 65
- [16] Coomer B J, Goss J P, Jones R, Briddon P R and Oberg S 2001 *Diamond Relat. Mater.* at press
- [17] Twitchen D J, Newton M E, Baker J M, Banholzer W F and Anthony T R 1999 *Diamond Relat. Mater.* **8** 1101
- [18] Davies G 1974 *Proc. R. Soc. A* **336** 507
- [19] Walker J 1975 *Lattice Defects in Semiconductors 1974 (Inst. Phys. Conf. Ser. 23)* (Bristol: Institute of Physics Publishing) p 317
- [20] Walker J 1997 *Rep. Prog. Phys.* **4** 1605
- [21] Steeds J W, Charles S, Davis T J, Gilmore A, Hayes J, Pickard D and Butler J E 1999 *Diamond Relat. Mater.* **8** 94
- [22] Steeds J W, Davis T J, Charles S, Hayes J M and Butler J E 1999 *Diamond Relat. Mater.* **8** 1847
- [23] Aria N, Takeda S and Kohyama M 1997 *Phys. Rev. Lett.* **78** 4265